Quantum Lifshitz criticality in a frustrated two-dimensional XY model

Yaroslav A. Kharkov,[1,2] Jaan Oitmaa,[1] and Oleg P. Sushkov[1]
[1]*School of Physics, University of New South Wales, Sydney 2052, Australia*
[2]*Joint Quantum Institute and Joint Center for Quantum Information and Computer Science, NIST/University of Maryland, College Park, Maryland 20742, USA*

(Received 21 October 2019; revised manuscript received 13 December 2019; published 9 January 2020)

Antiferromagnetic quantum spin systems can exhibit a transition between collinear and spiral ground states, driven by frustration. Classically this is a smooth crossover and the crossover point is termed a Lifshitz point. Quantum fluctuations change the nature of the transition. In particular, it has been argued previously that in the two-dimensional (2D) case a spin liquid (SL) state is developed in the vicinity of the Lifshitz point, termed a Lifshitz SL. In the present work, using a field theory approach, we solve the Lifshitz quantum phase transition problem for the 2D frustrated XY model. Specifically, we show that, unlike the $SU(2)$ symmetric Lifshitz case, in the XY model, the SL exists only at the critical point. At zero temperature we calculate nonuniversal critical exponents in the Néel and in the spin spiral state and relate these to properties of the SL. We also solve the transition problem at a finite temperature and discuss the role of topological excitations.

DOI: 10.1103/PhysRevB.101.035114

I. INTRODUCTION

The Lifshitz point is the classical (nonquantum) crossover between a collinear antiferromagnet and a spin spiral state. The crossover is driven by frustration. Some time ago Ioffe and Larkin pointed out that if a frustrated 2D antiferromagnet is tuned to the Lifshitz point, long wavelength quantum fluctuations destroy the long-range order and lead to the formation of a quantum disordered phase, a spin liquid (SL). [1] In the present paper, we term this phase a Lifshitz SL. It has properties which are different from other known types of SL. Locally it maintains antiferromagnetic or spin spiral correlations. For this reason quantum field theory is the most natural technique to describe the state, and this technique was used already in the pioneering work [1]. After the first work the idea of Lifshitz quantum criticality and Lifshitz SL was almost forgotten. However recently it has attracted more attention. Lifshitz quantum criticality arises in frustrated quantum magnets with competing interactions [2–6] and in underdoped cuprates where the effective frustration is due to itinerant holes [7,8]. Interestingly, the XY-type Lifshitz field theories arise also in Rokhsar-Kivelson dimer models [2,9], as well as in liquid crystals [10], Bose-Einstein condensates of ultracold atoms [11], and even in some cosmological models [12,13]. A Lifshitz point in a classical frustrated XY model at a finite temperature was also considered in Ref. [14] Lifshitz-type quantum criticality may arise in thin films of manganite oxide materials Tb(Dy)MnO_3, where the criticality could be tuned by La-doping or pressure [15–18].

In the present work we study 2D frustrated magnets with competing interactions and solve the problem of a Lifshitz quantum phase transition in the 2D frustrated XY model. We derive a field theoretical description for the $O(2)$ symmetric model in the vicinity of the Lifshitz transition. This allows us to calculate nonunversal critical exponents in the Néel and in the spin spiral state and relate these to properties of the SL. We also study the Lifshitz transition at a finite temperature, accounting for both quantum and thermal fluctuations. We discuss the relative importance of the perturbative and the topological (vortex) excitations. We also underline differences between Lifshitz criticalities for the XY and the SU(2)-symmetric case.

The paper is organized as follows. In Sec. II, we discuss the J_1-J_3 Heisenberg model on the square lattice, $S = 1/2$, as an example of Lifshitz criticality. Here we present results of numerical series expansion calculations that motivate further analytical analysis. Section III presents analytical solution of the problem at zero temperature. finite-temperature properties are considered in Sec. IV. Section V summarizes our conclusions.

II. J_1-J_3 MODEL, SERIES EXPANSIONS

Before presenting the general solution in the framework of a quantum field theory, we consider a specific lattice model. One of the simplest 2D spin systems with frustration induced by competing interactions is J_1-J_3 Heisenberg antiferromagnet on the square lattice,

$$H = J_1 \sum_{\alpha\langle ij\rangle} S_i^\alpha S_j^\alpha + J_3 \sum_{\alpha\langle\langle ij\rangle\rangle} S_i^\alpha S_j^\alpha, \tag{1}$$

where $\boldsymbol{S}_i$ is spin 1/2 at the lattice site i. Antiferromagnetic interactions, $J_{1,3} > 0$, account for the nearest neighbor sites, and the third neighbor sites. If the summation over α is performed over all components of spin, $\alpha = x, y, z$, the model is SU(2)-symmetric, or $O(3)$-symmetric. The case $\alpha = x, y$ corresponds to the XY model, with $O(2)$ symmetry.

Frustrated J_1-J_2 and J_1-J_2-J_3 models have been discussed in numerous studies, see, e.g., Refs. [19–25]. In the J_1-J_2 model the nontrivial regime is realized around $J_2/J_1 \sim 0.5$. In this regime energies of the Néel state, the spin spiral

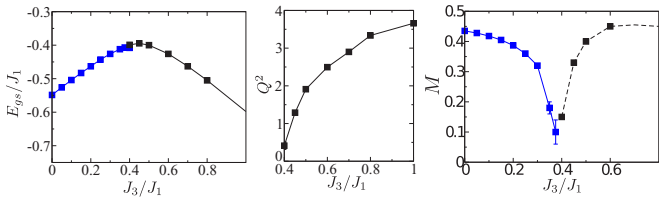

FIG. 1. The $O(2)$ J_1-J_3 model. At $J_3/J_1 < 0.4$. the ground state is the Néel state, and at $J_3/J_1 > 0.4$ the ground state is the spin spiral state. The spin liquid is realized at one point, $J_3/J_1 \approx 0.4$. (a) Energy of the ground state vs J_3/J_1. (b) The spin spiral wave vector squared vs J_3/J_1. (c) Static magnetization M vs J_3/J_1.

state, and the spin stripe state are close. The spin stripe state "spoils" the situation. It has very different short-range spin structure and this structure is strongly mixed up by quantum fluctuations. Therefore the J_1-J_2 model definitely does not belong to the Lifshitz class. However in J_1-J_3 model the situation is different. In the classical limit, $S \gg 1$, there is a Lifshitz point at $J_3 = J_1/4$ with a smooth formation of the spin spiral at $J_3 > J_1/4$. The spin stripe phase with the different short-range order has a significantly higher energy, and does not play a role at low temperature. So the J_1-J_3 model likely belongs to the Lifshitz class.

We have performed extensive series expansion calculations [26] both in the Néel phase and the spin-spiral phase. Unfortunately the series expansion method is not able to probe properties of the SL phase directly. However, the method allows us to find the range of parameters where the SL exists. In the Néel phase the series starts from the simple Ising antiferomagnetic state. In the spin spiral phase the calculation is more tricky. We first impose a classical diagonal spiral with some wave vector Q and find the total energy of this state $E(Q)$. This includes the classical energy and the quantum corrections calculated by means of series expansions. We perform this calculations for many values of Q and then find numerically the minimum of $E(Q)$. Such procedure gives us the ground-state energy E_{gs} and the physical wave vector Q. Plots of the ground-state energy E_{gs}, the spiral vector Q, and the static on-site magnetization M for the XY J_1-J_3 model are presented in Fig. 1. For comparison, in Fig. 2, we present the same quantities calculated in Ref. [6] for the $O(3)$ J_1-J_3 model.

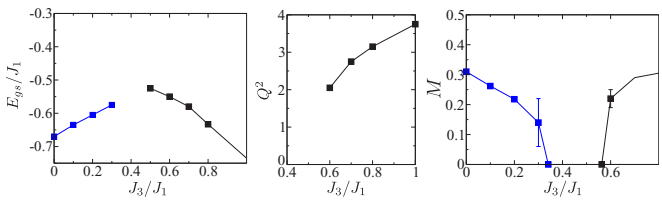

FIG. 2. The $O(3)$ J_1-J_3 model, results of Ref. [6] At $J_3/J_1 < 0.33$, the ground state is the Néel state, and at $J_3/J_1 > 0.55$ the ground state is the spin spiral state. The quantum disordered (spin liquid) phase is realized within the range $0.33 < J_3/J_1 < 0.55$. (a) Energy of the ground state vs J_3/J_1. (b) The spin spiral wave vector squared vs J_3/J_1. (c) Static magnetization vs J_3/J_1.

Note that according to our series calculations the period of the incommensurate spin spiral is quite long. For example, $Q^2 = 2$ implies that $Q_x = Q_y = 1 = 1/(2\pi)$r.l.u. So, the period in each direction is $2\pi \approx 6$ lattice spacing. While the series expansion method does not have a problem with this, it can be quite hard to obtain such a long period in a finite cluster calculation. Moreover, the ground state is fourfold degenerate, $\boldsymbol{Q} = \frac{1}{\sqrt{2}}(\pm Q, \pm Q)$. This is on the top of the continuous O(N) degeneracy that results in a well understood rotational tower of quantum states in a finite system [27,28]. In the spiral case, the continuous group tower must consist of fourfold split (or degenerate) states due to the Q degeneracy, and the splitting depends on the geometry of the cluster. It could be nontrivial to disentangle such a spectrum in a finite size cluster numerically.

Concluding this section, the most important qualitative difference between $O(3)$ and $O(2)$ is the size of the "window" in the parameter space occupied by the SL phase. In the $O(3)$ case this is finite interval and in the $O(2)$ case it is likely that the interval shrinks to a point. Remarkably the problem of the critical behavior of the $O(2)$ Lifshitz model can be solved exactly. Now we proceed to the solution.

III. ZERO-TEMPERATURE SOLUTION

In the vicinity of the Lifshitz point, the spin dynamics is described by an effective nonlinear σ model with the Lagrangian [1]

$$\mathcal{L} = \frac{\chi_\perp}{2}(\partial_t n_\mu)^2 - \frac{1}{2} n_\mu K(\partial_i) n_\mu \,. \tag{2}$$

Here, n_μ is the vector of staggered magnetization, with $\boldsymbol{n}^2 = 1$, ∂_i are the spatial gradients ($i = x, y$), $\chi_\perp$ is the transverse magnetic susceptibility. The general form of the "elastic energy" operator $K(\partial_i)$ assuming that the n-field is sufficiently smooth is

$$K(\partial_i) = -\rho(\partial_i)^2 + b_1\left(\partial_x^4 + \partial_y^4\right) + 2b_2\partial_x^2\partial_y^2 + \mathcal{O}\left(\partial_i^6\right). \tag{3}$$

The elastic energy has been derived in Ref. [1], see also Refs. [6,31]. The energy arises after rewriting Hamiltonian (1) in the Fourier representation and performing expansion $\cos q = 1 - q^2/2 + q^4/24$ up to the fourth power in momentum. The terms $\cos q$ ($\cos 2q$) originate from J_1 (J_3) Heisenberg interactions. The kinematic form of the Lagrangian (2) is dictated by global symmetries of the system. In the $O(3)$ case, the vector $\boldsymbol{n}$ has three components and in the $O(2)$ case two components. Hereafter, we consider $O(2)$ and hence the vector can be parameterized by the single angle θ

$$\boldsymbol{n} = (\cos\theta, \sin\theta). \tag{4}$$

The spin stiffness ρ is the tuning parameter that drives the system across the Lifshitz transition. The spin stiffness is positive in the Néel phase, negative in the spiral phase and vanishes at the Lifshitz point. The fourth-order spatial derivative b terms are necessary for stabilisation of the spiral order at negative ρ, and we assume $b_{1,2} > 0$.

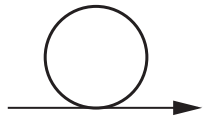

FIG. 3. Single loop self-energy diagram for θ-field generated by the quartic term in Eq. (5).

The Lagrangian (2) can be rewritten in terms of the angle θ:

$$\mathcal{L} = \chi_\perp \frac{(\partial_t\theta)^2}{2} - \frac{\rho(\partial_i\theta)^2}{2} - \frac{b_1}{2}\Big[\left(\partial_x^2\theta\right)^2 + \left(\partial_y^2\theta\right)^2 + (\partial_x\theta)^4 + (\partial_y\theta)^4\Big] - b_2\Big[\left(\partial_{xy}^2\theta\right)^2 + (\partial_x\theta)^2(\partial_y\theta)^2\Big]. \tag{5}$$

Classically the ground state of this Lagrangian is the collinear Néel state at $\rho > 0$, $\theta = \text{const}$ and the ground state is the spin spiral at $\rho < 0$, $\theta = \boldsymbol{Q}\boldsymbol{r}$, where $\boldsymbol{Q}$ is the wave vector of the spiral. For $b_1 \leqslant b_2$, the spiral wave vector is directed along x or y, and for $b_1 > b_2$, the wave vector is directed along the main diagonals.

$$\begin{aligned} b_1 \leqslant b_2: \quad & \boldsymbol{Q} = (\pm Q, 0), (0, \pm Q), \\ & Q^2 = |\rho|/(2b_1), \\ b_1 > b_2: \quad & \boldsymbol{Q} = \frac{1}{\sqrt{2}}(\pm Q, \pm Q), \quad \frac{1}{\sqrt{2}}(\pm Q, \mp Q), \\ & Q^2 = |\rho|/(b_1 + b_2). \end{aligned} \tag{6}$$

Parameters of the effective Lagrangians (2) and (5) can be expressed in terms of the parameters of the Heisenberg model. These are expansions in powers of spin S. For the J_1-J_3 Heisenberg model on the square lattice in the leading order in S, the parameters are [1,6]

$$\begin{aligned} \rho &= S^2(J_1 - 4J_3), \\ b_1 &= \frac{S^2}{24}(-J_1 + 16J_3), \\ b_2 &= 0, \\ \chi_\perp &= 1/(8J_1). \end{aligned} \tag{7}$$

The Lagrangian (5) contains quartic in θ terms. These terms lead to the self-energy of the field θ. The single loop self-energy diagram is shown in Fig. 3. The self-energy Fig. 3 has an ultraviolet part that is not singular at $\rho \to 0$ and it also has an infrared part singular at $\rho \to 0$. The ultraviolet part just gives subleading corrections in S to Eqs. (7). For example, the quartic terms result in the positive ultraviolet correction to ρ which extends the region of the Neel phase in Fig. 1. The Lifshiz point shifts to $J_3/J_1 \approx 0.4$ from the classical Lifshits point $J_3/J_1 = 0.25$ that follows from Eqs. (7). It is interesting to note that quantum fluctuations extend the region of the Néel phase, this is the general property of Lifshitz criticality. [6] On the other hand in the J_1-J_2 model quantum fluctuations shrink the region of the Néel phase. The classical critical point is $J_2/J_1 = 0.5$ and the quantum critical point is $J_2/J_1 = 0.38$ [20]. This observation confirms our point that the J_1-J_2 model does not belong to the Lifshitz class. Thus the renormalization due to the ultraviolet part of Fig. 3 significantly changes parameters of the model and shifts the position of the Lifshitz critical point. However, from the point of view of a field theory, the ultraviolet part of Fig. 3 can be renormalized out (eliminated).

The infrared part of the self energy is more interesting, as it influences critical properties, and we discuss this point below. The transverse susceptibility $\chi_\perp$ does not have an infrared divergent correction, and in the single loop approximation, Fig. 3, the correction is actually zero. Therefore hereafter we set $\chi_\perp = 1$ and hence use dimensionless parameters

$$\begin{aligned} \rho &\to \chi_\perp \rho, \\ b_{1,2} &\to \chi_\perp b_{1,2}, \\ T &\to \chi_\perp T. \end{aligned} \tag{8}$$

The last line defines a dimensionless temperature that we use in the next section.

The values of the coefficients b_1 and b_2 depend on the specific choice of the lattice model. The special case $b_1 = b_2$ corresponds to the situation when the ground-state energy is degenerate with respect to the direction of $\boldsymbol{Q}$. In this degenerate case, one has to account for higher-order terms in the powers of the spatial gradients $\mathcal{O}(\partial_i^6)$ in the expansion of the elastic energy $K(\partial_i)$. In this work, we assume that the system is far away from the degeneracy point, $b_1 = b_2$.

A. Spin stiffness renormalization

Let us approach the Lifshitz point from the Néel phase, $\rho > 0$. Quadratic in θ terms of the Lagrangian (5) result in the following dispersion:

$$\omega_q = \sqrt{\rho q^2 + b_1\left(q_x^4 + q_y^4\right) + 2b_2 q_x^2 q_y^2}, \tag{9}$$

where q is the momentum. At the Lifshitz point, $\rho = 0$, the dispersion is quadratic in momentum, and the dynamical critical exponent is $z = 2$,

$$\omega_{0q} = \sqrt{b_1\left(q_x^4 + q_y^4\right) + 2b_2 q_x^2 q_y^2}. \tag{10}$$

To calculate the self-energy Fig. 3, we decouple the nonlinear terms in the Lagrangian (5)

$$(\partial_i\theta)^4 \to 6(\partial_i\theta)^2\langle(\partial_i\theta)^2\rangle = 3(\partial_i\theta)^2 \int \frac{d^2q}{(2\pi)^2}\frac{q_i^2}{\omega_q}. \tag{11}$$

Thus the self-energy results in a correction to the spin stiffness. First we perform the ultraviolet renormalization. To do so consider the Lifshitz point, $\rho = 0$. Here the correction is

$$\Delta\rho = \left(3b_1 + \frac{b_2}{2}\right)\int \frac{d^2q}{(2\pi)^2}\frac{q_x^2}{\omega_{0q}}. \tag{12}$$

The integral is convergent in the infrared limit ($q \to 0$) in spite of the quadratic dispersion. Hence, $\Delta\rho$ is just a constant that has to be added to the relation (7). We absorb this shift in the definition of ρ. Away from the Lifshitz point in the Néel phase the self-energy leads to a logarithmic renormalization of the spin stiffness, $\rho \to \rho_r$. Similar to (12), we find

$$\rho_r = \rho + \left(3b_1 + \frac{b_2}{2}\right)\int \frac{d^2q}{(2\pi)^2} q_x^2\left[\frac{1}{\omega_q} - \frac{1}{\omega_{0q}}\right]. \tag{13}$$

For self-consistency in the dispersion ω_q in this formula, we must replace $\rho \to \rho_r$, see Eq. (9). Evaluation of the integral in (13) with logarithmic accuracy is straightforward. This leads to the following equation for the renormalized spin stiffness ρ_r:

$$\rho_r = \frac{\rho}{1 + \frac{3\kappa_0}{8\pi\sqrt{b_1}}\left(1 + \frac{b_2}{6b_1}\right)\ln\left(\frac{\Lambda^2 b_1}{|\rho_r|}\right)}. \tag{14}$$

Here, $\Lambda \sim \pi/a$ is the ultraviolet momentum cutoff, a is the lattice spacing, and the number κ is the following angular integral:

$$\kappa_0 = \int_0^{2\pi} \frac{d\alpha/(2\pi)\,\cos^2\alpha}{[(\cos^4\alpha + \sin^4\alpha) + 2(b_2/b_1)\sin^2\alpha\cos^2\alpha]^{3/2}}. \tag{15}$$

The logarithmic correction to the spin stiffness can not depend on the sign of ρ, so (14) is valid also for $\rho < 0$. This point is obvious since the logarithmic correction comes from quantum fluctuations in the momentum range $Q \sim \sqrt{|\rho|/b_1} < q < \Lambda$. This range is insensitive to formation of the spin spiral. This implies that in Eqs. (6) one must replace $\rho \to \rho_r$ and the correct scaling of the wave vector is

$$Q \propto \sqrt{\rho_r} \propto \sqrt{\frac{J_3 - J_{3c}}{1 + A\ln\left(\frac{B}{J_3 - J_{3c}}\right)}}, \tag{16}$$

where the constants A and B are given by Eq. (14). So, there is a logarithmic correction to the power scaling of Q. Besides the general scaling arguments one can check the relation $Q \propto \sqrt{\rho_r}$ by a detailed calculation. To do so, we substitute $\theta = \boldsymbol{Qr} + \phi$ in the Lagrangian (5) and expand it up to cubic terms $(\partial_i\phi)^3$. A straightforward decoupling procedure $(\partial_i\phi)^3 \to 3(\partial_i\phi)\langle(\partial_i\phi)^2\rangle$ leads directly to Eq. (14). The logarithmic correction in Eq. (16) is small. Therefore the deviation of Fig. 1(b) from a straight line is due to the higher powers of $J_3 - J_{3c}$ that cannot be captured by the field theory.

It is interesting to note that nonlinear terms in the Lagrangian (5) do not renormalize the higher derivative terms $b_{1,2}(\partial^2\theta)^2$. Such corrections can only be generated by subleading terms, e.g., $(\partial^2\theta)^4$ or $(\partial^2\theta)^2(\partial\theta)^2$.

In the spin spiral phase it is convenient to describe excitations in terms of the field ϕ. The substitution $\theta = \boldsymbol{Qr} + \phi$ in the Lagrangian (5) results in the following quadratic form:

$$\frac{1}{2}\widetilde{\rho}_{ij}\partial_i\phi\partial_j\phi + \frac{b_1}{2}[(\partial_{xx}\phi)^2 + (\partial_{yy}\phi)^2] + b_2(\partial_{xy}\phi)^2. \tag{17}$$

Hence the effective spin stiffness tensor $\widetilde{\rho}_{ij}$, which determines the spectrum of excitations in the spin spiral phase, reads

$$\widetilde{\rho}_{ij} = 2|\rho_r|\begin{pmatrix} 1 & 0 \\ 0 & \frac{b_2}{b_1} - 1 \end{pmatrix}, \quad b_1 \leqslant b_2;$$

$$\widetilde{\rho}_{ij} = 2|\rho_r|\begin{pmatrix} \frac{b_1}{b_1+b_2} & \frac{b_2}{b_1+b_2} \\ \frac{b_2}{b_1+b_2} & \frac{b_1}{b_1+b_2} \end{pmatrix}, \quad b_1 > b_2. \tag{18}$$

Hence the excitation spectrum in the spin spiral phase is

$$\widetilde{\omega}_q = \sqrt{\widetilde{\rho}_{ij}q_iq_j + b_1\left(q_x^4 + q_y^4\right) + 2b_2q_x^2q_y^2}. \tag{19}$$

B. Spin-spin correlator

From Eq. (9), we conclude that the phase fluctuation in the Néel phase reads

$$\langle\theta^2(r)\rangle - \langle\theta(r)\rangle^2 = \int \frac{d^2q}{(2\pi)^2}\frac{1}{2\omega_q}. \tag{20}$$

The fluctuation remains finite everywhere except of the point $\rho = 0$ where the integral in (20) is infrared divergent. This confirms the hint given by Fig. 1(c) that the spin liquid is realized only at one point. Everywhere else the long-range order is preserved. To calculate the spin-spin correlator in the SL phase we follow the method of Ref. [2]. The equal time correlator of the $\boldsymbol{n}$-field can be expressed in terms of the θ correlation function, $G(x-y) = \langle\theta(x)\theta(y)\rangle$:

$$C(r) = \langle n_\mu(r)n_\mu(0)\rangle = Re\langle e^{i\theta(r)}e^{-i\theta(0)}\rangle = e^{G(r)-G(0)}. \tag{21}$$

The θ-field Green's function reads

$$G(r) = \langle\theta(r)\theta(0)\rangle = \int \frac{d^2q}{(2\pi)^2}\frac{e^{i\boldsymbol{qr}}}{2\omega_{0q}}. \tag{22}$$

Hence

$$\begin{aligned} G(r) - G(0) &= \int_0^\Lambda \frac{d^2q}{(2\pi)^2}\frac{e^{i\boldsymbol{qr}} - 1}{2\omega_{0q}} \\ &= \int_0^{\Lambda r}\frac{d\eta}{\eta}\int_0^{2\pi} \\ &\quad \times \frac{d\alpha[e^{i\eta\cos(\psi-\alpha)} - 1]/(8\pi^2\sqrt{b_1})}{\sqrt{(\cos^4\alpha + \sin^4\alpha) + 2(b_2/b_1)\sin^2\alpha\cos^2\alpha}} \end{aligned} \tag{23}$$

Here the angle ψ describes the orientation of the radius vector $\boldsymbol{r} = r(\cos\psi, \sin\psi)$ in the 2D plane $\{x, y\}$. The first term in the square brackets is convergent at large η while the second term is logarithmically divergent. Therefore the first term just provides the lower limit of integration, $\eta \sim 1$, for the second one. Hence, at $\Lambda r \gg 1$,

$$G(r) - G(0) \approx -\frac{\kappa_1}{4\pi\sqrt{b_1}}\int_1^{\Lambda r}\frac{d\eta}{\eta} = -\zeta\ln(\Lambda r)\,, \tag{24}$$

where

$$\zeta = \frac{\kappa_1}{4\pi\sqrt{b_1}},$$

$$\kappa_1 = \int_0^{2\pi}\frac{d\alpha/(2\pi)}{\sqrt{(\cos^4\alpha + \sin^4\alpha) + 2(b_2/b_1)\sin^2\alpha\cos^2\alpha}}. \tag{25}$$

Thus the spin-spin correlator at the critical point, $\rho \to 0$, decays algebraically

$$C(r) = \left(\frac{1}{\Lambda r}\right)^\zeta. \tag{26}$$

Interestingly, this correlator decay for the XY-Lifshitz spin liquid is similar to that in the dimer models at the Rokhsar-Kivelson critical point [2,29].

C. Static magnetization

The staggered magnetization in the Neel phase, $\rho > 0$, is

$$\langle n_x \rangle = Re\langle e^{i\theta} \rangle = e^{-(\langle\theta^2\rangle - \langle\theta\rangle^2)/2} . \quad (27)$$

We choose the x-axis as the direction of spontaneous symmetry breaking in the Neel phase. The fluctuation of phase θ is given by Eq. (20). According to Eq. (9) there is a regime crossover at

$$q_{\min} \sim \sqrt{\rho_r / b} . \quad (28)$$

At $q > q_{\min}$ the dispersion is quadratic in q, and at $q < q_{\min}$ the dispersion is linear in q. Therefore, $q_{\min}$ is the infrared cutoff in the logarithmically divergent integral in (20). Hence

$$\langle\theta^2\rangle - \langle\theta\rangle^2 = \int_{qmin}^{\Lambda} \frac{d^2q}{(2\pi)^2} \frac{1}{2\omega_q} = \zeta \ln(\Lambda/q_{\min}) . \quad (29)$$

This results in the following critical behavior of the static magnetization

$$M \propto \langle n_x \rangle \propto \rho_r^{\zeta/4} . \quad (30)$$

It is easy to check that the static magnetization in the spin-spiral phase has the same scaling $M \propto |\rho_r|^{\zeta/4}$.

It would be interesting to understand how an external magnetic field and a quenched disorder can influence the derived behavior. Obviously a weak magnetic field orthogonal to the xy plane does not influence Goldstone excitations and hence does not influence the behavior. On the other hand a field in the plane, say along the x axis, aligns the staggered magnetization along the y axis and opens a gap in the spectrum of excitations in the collinear phase. Most likely such a field would change the continuous Lifshitz quantum phase transition to a weak first-order transition.

A weak quenched disorder, say removal of a small fraction of spins, is a more complex issue. We believe that the $O(3)$ case, where SL exists in a finite window of J_3/J_1, will not be significantly affected by the disorder. On the other hand in the $O(2)$ case this is not true. In this case the SL exists only in Lifshitz point where excitations are gapless with quadratic dispersion. Obviously the disorder is not important deep in the collinear phase and deep in the spin spiral phase. However in a vicinity of the Lifshitz point it could effect the system. A likely scenario is a SL with superimposed spin glass component in a narrow vicinity of the Lifshitz point. Analysis of such state is a complex problem outside of the scope of the present work.

Thus we come to the following conclusions of this section. (i) The SL is realized only at the critical point, $\rho_r = 0$. (ii) The spin-spin correlator in the SL phase decays algebraically $\propto r^{-\zeta}$. (iii) The static magnetization away from the SL point scales as $\rho_r^{\zeta/4}$. The critical index is not a universal number, but it depends on parameters of the system, see Eq. (25). For the J_1-J_3 model, the critical point is $J_{3c} \approx 0.4$, see Fig. 1(c). Hence using Eq. (7), we estimate $\zeta/4 \approx 0.25$. (iv) Because of the logarithmic correction in Eq. (14) the critical scaling is not just a power, but there is a logarithmic dependence. (v) The incommensurate wave vector scaling in the spin spiral phase also has a logarithmic correction, Eq. (16).

IV. FINITE-TEMPERATURE PROPERTIES

A. Spin stiffness renormalization

In this section, we consider the effects of finite temperature T on Lifshitz criticality. We assume that the temperature is much smaller than the energy ultraviolet cutoff, $T \ll \sqrt{b}\Lambda^2$, but it can be larger or comparable with ρ. It is obvious that with these conditions temperature does not influence the ultraviolet renormalization (12). However, the infrared renormalization (13) is changed. The $1/\omega_q$ term in the square brackets in (13) should be replaced by a term containing a bosonic occupation number factor $\frac{1}{\omega_q} \to \frac{1}{\omega_q}(1 + 2n_q)$, where

$$n_q = \frac{1}{e^{\omega_q/T} - 1} . \quad (31)$$

Hence Eq. (13) modified for the case of finite T reads

$$\rho_r = \rho + \left(3b_1 + \frac{b_2}{2}\right) \int \frac{d^2q}{(2\pi)^2} q_x^2 \left[\frac{1}{\omega_q} - \frac{1}{\omega_{0q}}\right] + \left(3b_1 + \frac{b_2}{2}\right) \int \frac{d^2q}{(2\pi)^2} q_x^2 \frac{2n_q}{\omega_q} . \quad (32)$$

This equation is written for the Néel phase. For low temperature, $T \lesssim \rho$, the last line in Eq. (32) is negligible and we return back to (13). However, for $\rho \ll T \ll \sqrt{b}\Lambda^2$ temperature is significant and evaluation of (32) gives

$$\rho_r = \frac{\rho + \frac{3T\kappa_2}{2\pi}\left(1 + \frac{b_2}{6b_1}\right) \ln\left(\frac{\sqrt{b_1}T}{|\rho_r|}\right)}{1 + \frac{3\kappa_0}{8\pi\sqrt{b_1}}\left(1 + \frac{b_2}{6b_1}\right) \ln\left(\frac{\Lambda^2 b_1}{|\rho_r|}\right)} , \quad (33)$$

where

$$\kappa_2 = \int_0^{2\pi} \frac{d\alpha/(2\pi)\ \cos^2\alpha}{(\cos^4\alpha + \sin^4\alpha) + 2(b_2/b_1)\sin^2\alpha\cos^2\alpha} . \quad (34)$$

An equation similar to (33) was obtained in Ref.[29] for a particular case $\rho = 0$. Note that Eq. (33) has a positive solution, $\rho_r > 0$, for small negative ρ. This means that the stability region of the commensurate fluctuating "Neel" phase at finite temperatures extends towards negative ρ, as shown in the phase diagram in Fig. 4.

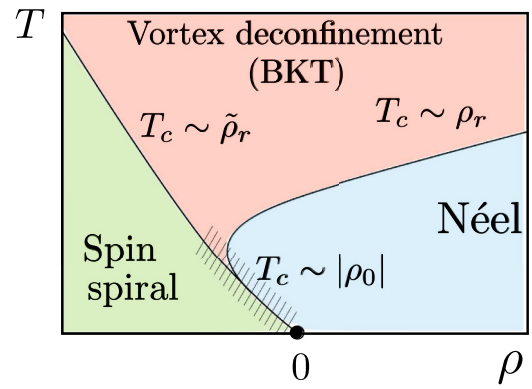

FIG. 4. Sketch of the T-ρ phase diagrams of the quantum Lifshitz transition in XY model for a finite system size L. Neel and Spin spiral phases at $T > 0$ possess a quasi-long-range order and algebraic spin-spin correlations.

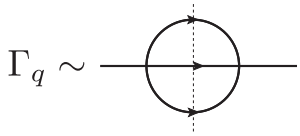

FIG. 5. Two-loop self-energy diagram that generates width of the magnon.

B. Magnon lifetime effect

When considering Eq. (33) at very small ρ_r we will face a serious problem. The equation (33) does not have a solution $\rho_r = 0$. Hence the transition line in Fig. 4 between the fluctuating Néel state and the fluctuating spin spiral state is undetermined. To resolve this problem, we need to consider perturbative and nonperturbative (topological) fluctuations. In this section, we consider perturbative fluctuations. Equation (33) is derived in the single loop approximation, see Fig. 3. In this approximation, the self-energy does not have an imaginary part. The imaginary part arises due to the double loop diagram shown in Fig. 5. The four-magnon vertex in Fig. 5 is generated by quartic terms $b(\partial\theta)^4$ in Eq. (5). In what follows, we denote by q the momentum of the probe magnon, and k_1, k_2, k_3 are momenta of magnons from the heat bath. There are three types of the scattering processes contributing to the width: (i) decay: $q = k_1 + k_2 + k_3$, (ii) Raman: $q + k_1 = k_2 + k_3$, and (iii) fusion: $q + k_1 + k_2 = k_3$. We consider the most important Raman process, the corresponding width reads (see, e.g., Ref. [30])

$$\Gamma_q \sim \frac{(1-e^{-\omega_q/T})}{\omega_q} b^2 q^2 \int \frac{d^2k_1}{2\omega_1}\frac{d^2k_2}{2\omega_2}\frac{d^2k_3}{2\omega_3} k_1^2 k_2^2 k_3^2 \times n_1(1+n_2)(1+n_3)\,\delta(\omega_q+\omega_1-\omega_2-\omega_3) \times \delta^{(2)}(\boldsymbol{q}+\boldsymbol{k}_1-\boldsymbol{k}_2-\boldsymbol{k}_3)\,. \tag{35}$$

We are interested in the case $\rho_r = 0$, hence the dispersion is $\omega_q = \sqrt{b}q^2 \ll T$, $\omega_i = \sqrt{b}k_i^2 \ll T$. The occupation numbers can be replaced as $n_i \to T/\omega_i$. Evaluation of the integral in (35) is straightforward, the result is

$$\Gamma_q \sim \frac{T^2}{\sqrt{b}}\frac{q^2}{\omega_q^2}\,. \tag{36}$$

This estimate is valid if $\Gamma_q \ll \omega_q$. At very small $q \to 0$ this condition is violated and hence in the right hand side of (36) we have to replace $\omega_q \to \Gamma_q$. This immediately gives the following estimate for Γ_q at very small q

$$\Gamma_q \sim \frac{T^{2/3}}{b^{1/6}} q^{2/3}\,. \tag{37}$$

This width results in the effective infrared cutoff in the q integration in the last line of Eq. (32). Hence, with account of the width, Eq. (33) is replaced by

$$\rho_r = \frac{\rho + \frac{3T\kappa_2}{2\pi}\ln\sqrt{b}}{1+\frac{3\kappa_0}{8\pi\sqrt{b_1}}\left(1+\frac{b_2}{6b_1}\right)\ln\left(\frac{\Lambda^2 b_1}{|\rho_r|}\right)} \to \frac{\rho + \mathcal{C}T}{1+\frac{3\kappa_0}{8\pi\sqrt{b_1}}\left(1+\frac{b_2}{6b_1}\right)\ln\left(\frac{\Lambda^2 b_1}{|\rho_r|}\right)}. \tag{38}$$

The q integral in the numerator of this equation has been calculated with logarithmic accuracy, $\ln(q_T/q_{\min}) \gg 1$, where $q_{\min}$ is the lifetime infrared cutoff that follows from Eq. (37). However, in the end, the logarithm proved to be not large. Therefore, we must replace it by a constant $\mathcal{C}$ that we cannot calculate within accuracy of the method. We can only claim that the constant is positive since the integral in the second line of Eq. (32) is positive. The transition line in Fig. 4 between the fluctuating Néel state and the fluctuating spin spiral state is given by the condition $\rho_r = 0$, that results in the condition

$$\rho = -\mathcal{C}T. \tag{39}$$

C. Finite-temperature spin-spin correlators

Let us consider the spin-spin correlator at the transition line $\rho_r = 0$, see Fig. 4. At a finite temperature, Eq. (23) is transformed to

$$G(r) - G(0) = \int_0^\Lambda \frac{d^2q}{(2\pi)^2}\frac{e^{i\boldsymbol{qr}}-1}{2\omega_{0q}}(1+2n_q) \approx T\int_0^{q_T}\frac{d^2q}{(2\pi)^2}\frac{e^{i\boldsymbol{qr}}-1}{\omega_{0q}^2} + \int_{q_T}^\Lambda \frac{d^2q}{(2\pi)^2}\frac{e^{i\boldsymbol{qr}}-1}{2\omega_{0q}}, \tag{40}$$

where $q_T = \sqrt{T}/b^{1/4}$. The first integral in this equation is infrared logarithmic divergent. As was discussed in the previous subsection the integral has to be regularized by the finite width, $\omega_{0q}^2 \to \omega_{0q}^2 + \Gamma_q^2$. Evaluation of the integrals in (40) is straightforward. At $q_T r \ll 1$ the correlator $C(r)$ decays with distance exactly like that in the zero temperature SL, Eq. (26), and at $q_T r \gg 1$ it very quickly decays to zero.

Away from the critical line, $\rho_r \neq 0$, at sufficiently large distances, $r \gg \sqrt{b/|\rho_r|}$, the spin-spin correlator decays according to the standard XY-model algebraic law

$$C(r) \propto \frac{1}{r^{T/(2\pi|\rho_r|)}}\,. \tag{41}$$

D. The role of vortices

A single vortex in the XY model has energy

$$E_{\text{vortex}} = E_{\text{core}} + \pi\rho\ln(L/a)\,, \tag{42}$$

where L is the size of the vortex (size of the sample) and E_{core} is the energy of the vortex core. Hence at a finite temperature, the free energy per vortex reads

$$F_{\text{vortex}} = E_{\text{core}} + \pi\rho\ln\left(\frac{L}{a}\right) - T\ln\left(\frac{L^2}{a^2}\right). \tag{43}$$

The third term in this equation is due to the entropy of the vortex gas $S_v \sim \ln(\frac{L^2}{a^2})$. In the usual unfrustrated XY model ($J_3 = 0$), the core energy $E_{\text{core}} \sim \rho \sim J_1$. Therefore the core energy does not play a significant role. In the limit $L \to \infty$ the vortex proliferation is energetically favorable ($F_{\text{vortex}} < 0$) at the temperatures above the BKT temperature $T > T_{\text{BKT}} = \frac{\pi}{2}\rho$. Formally near the Lifshitz point the situation is similar and we can write the following equation for T_{BKT}.

$$T_{\text{BKT}} = \frac{\pi}{2}|\rho|\,. \tag{44}$$

In particular $T_{\rm BKT} = 0$ at $\rho = 0$. Obviously Eq.(44) is not consistent with Fig. 4. The explanation is that this equation represent a rather formal statement. While at the Lifshitz point the spin stiffness is approaching zero due to frustration, $\rho \to 0$, the core energy remains finite, $E_{\rm core} \sim J_1$, see Ref. [31] According to Eq. (43) in the limit $L \to \infty$ and at $\rho = 0$ vortices proliferate at any nonzero temperature. This is consistent with Eq. (44). However, to make this point valid the entropy in Eq. (43) must dominate over the core energy, hence the sample size must be sufficiently large, $L > a \times e^{E_{\rm core}/2T}$. This can be a huge number, thousands, millions, or billions of lattice spacings that is never achieved in a real sample or in numerical experiments on a finite cluster.

Thus formally mathematically the transition line in Fig. 4 originating from $\rho = 0$ consists of two diverging phase boundary lines that are exponentially close to each other. The intermediate phase between the lines is the deconfined vortex phase. However, in a real sample, say 1000×1000 sites, still there is single transition line that at a certain temperature starts to diverge into two BKT lines as it is shown in Fig. 4. The position of the divergence point depends on the sample size dramatically, so the notion of the phase diagram near the divergence point is poorly defined.

To summarize this subsection, at finite system size and at a sufficiently low temperature the $O(2)$ topological excitations (vortices) are irrelevant near the Lifshitz point. This is because the vortex core energy remains finite even if the spin stiffness is zero. Interestingly, in the $O(3)$ case (isotropic Heisenberg model), the energy of the topological excitation, skyrmion, scales proportionally to the spin stiffness. Therefore, in this case, topological excitations are relevant near the Lifshitz point.

V. DISCUSSION AND CONCLUSION

We have considered the Lifshitz quantum phase transition problem for the 2D frustrated XY model. Here are the conclusions.

(i) We have performed numerical series expansion calculations for J_1-J_3 model on the square lattice ($S = 1/2$). The calculations indicate that the Lifshitz point behavior is very different for the XY- and for the $SU(2)$-symmetric versions of the model.

(ii) Motivated by the numerics we performed field theory analysis of the XY-Lifshitz criticality. This analysis results in the following points.

(iii) The Lifshitz spin liquid phase exists only at the Lifshitz point. This is different from the SU(2) case where the spin liquid phase occupies a finite interval in the parameter space.

(iv) At zero temperature we calculate nonuniversal critical exponents in the Néel and in the spin spiral state and relate them to properties of the spin liquid.

(v) We also solve the transition problem at a finite temperature, calculate the critical exponents, and discuss the role of the magnon lifetime on the finite-temperature critical behavior.

(vi) We show that the topological excitations are irrelevant at low temperature even near the critical point.

ACKNOWLEDGMENTS

We thank Matthew O'Brien for discussions and Anders Sandvik for important communications. The work has been supported by the Australian Research Council Project No. DP160103630.

[1] L. B. Ioffe and A. I. Larkin, J. Mod. Phys. B **02**, 203 (1988).
[2] E. Ardonne, P. Fendley, and E. Fradkin, Ann. Phys. **310**, 493 (2004).
[3] L. Capriotti and S. Sachdev, Phys. Rev. Lett. **93**, 257206 (2004).
[4] E. Fradkin, *Field Theories of Condensed Matter Physics*, 2nd ed. (Cambridge University Press, 2013).
[5] L. Balents and O. A. Starykh, Phys. Rev. Lett. **116**, 177201 (2016).
[6] Y. A. Kharkov, J. Oitmaa, and O. P. Sushkov, Phys. Rev. B **98**, 144420 (2018).
[7] Y. A. Kharkov and O. P. Sushkov, Phys. Rev. B **98**, 155118 (2018).
[8] Y. A. Kharkov and O. P. Sushkov, Phys. Rev. B **100**, 224510 (2019).
[9] D. S. Rokhsar and S. A. Kivelson, Phys. Rev. Lett. **61**, 2376 (1988).
[10] P. M. Chaikin, and T. C. Lubensky, *Principles of Condensed Matter Physics* (Cambridge University Press, 1995).
[11] H. C. Po and Q. Zhou, Nat. Commun. **6**, 8012 (2015).
[12] P. Horava, Phys. Rev. D **79**, 084008 (2009).
[13] C. Hoyos, B. S. Kim, and Y. Oz, J. High Energy Phys. 03 (2014) 029.
[14] H. Schenck, V. L. Pokrovsky, and T. Nattermann, Phys. Rev. Lett. **112**, 157201 (2014).
[15] T. Kimura, T. Goto, H. Shintani, K. Ishizaka, T. Arima, and Y. Tokura, Nature (London) **426**, 55 (2003).
[16] T. Goto, T. Kimura, G. Lawes, A. P. Ramirez, and Y. Tokura, Phys. Rev. Lett. **92**, 257201 (2004).
[17] K. Hirota, N. Kaneko, A. Nishizawa, and Y. Endoh, J. Phys. Soc. Jpn. **65**, 3736 (1996).
[18] A. I. Milstein and O. P. Sushkov, Phys. Rev. B **91**, 094417 (2015).
[19] J. Ferrer, Phys. Rev. B **47**, 8769 (1993).
[20] O. P. Sushkov, J. Oitmaa, and Zheng Weihong, Phys. Rev. B **63**, 104420 (2001).
[21] L. Capriotti, D. J. Scalapino, and S. R. White, Phys. Rev. Lett. **93**, 177004 (2004).
[22] P. Sindzingre, N. Shannon, and T. Momoi, J. Phys.: Conf. Ser. **200**, 022058 (2010).
[23] J. Reuther, P. Wölfle, R. Darradi, W. Brenig, M. Arlego, and J. Richter, Phys. Rev. B **83**, 064416 (2011).
[24] Z. Zhu, D. A. Huse, and S. R. White, Phys. Rev. Lett. **110**, 127205 (2013).
[25] R. F. Bishop, P. H. Y. Li, O. Götze, J. Richter, and C. E. Campbell, Phys. Rev. B **92**, 224434 (2015).

[26] J. Oitmaa, C. Hamer, and W. Zheng, *Series Expansion Methods for Strongly Interacting Lattice Models* (Cambridge University Press, 2006).
[27] P. W. Anderson, Phys. Rev. **86**, 694 (1952).
[28] G. Misguich, C. Lhuillier, M. Mambrini, and P. Sindzingre, Eur. Phys. J. B **26**, 167 (2002).
[29] P. Ghaemi, A. Vishwanath, and T. Senthil, Phys. Rev. B **72**, 024420 (2005).
[30] H. D. Scammell and O. P. Sushkov, Phys. Rev. B **95**, 024420 (2017).
[31] Y. A. Kharkov, O. P. Sushkov, and M. Mostovoy, Phys. Rev. Lett. **119**, 207201 (2017).